

**O.M. Korduban<sup>1</sup>, T.V. Kryshchuk<sup>1</sup>, V.O. Kandyba<sup>2</sup>, V.V. Trachevskii<sup>3</sup>**

## XPS STUDIES OF THE SURFACE OF TiO<sub>2</sub>:Ag NANOPOWDERS

<sup>1</sup> Vernadsky Institute of General and Inorganic Chemistry of National Academy of Sciences of Ukraine  
32/34 Academician Palladin Avenue, Kyiv, 03680, Ukraine, E-mail: tarkry@ukr.net

<sup>2</sup> Elettra – Sincrotrone Trieste SCpA  
SS14-km 163.5 in Area Science Park, Basovizza, 34012, Trieste, Italy

<sup>3</sup> Technical Center of National Academy of Sciences of Ukraine  
13 Pokrovskaya Str., Kyiv, 04070, Ukraine

*n-TiO<sub>2</sub> and n-TiO<sub>2</sub>:Ag nanopowders were synthesized by the method of electric explosion of wires (EEW). The doping of nanopowders took place during the explosion of titanium wire, on the surface of which an Ag<sub>2</sub>O layer of the appropriate mass was applied. The energy of the explosion was equal to  $E = 3.1 \cdot E_s$ , where  $E_s$  is the energy of sublimation of the metal. Based on the synthesized nanopowders, mesoporous n-TiO<sub>2</sub> and n-TiO<sub>2</sub>:Ag films were formed. The phase composition of the surface of several series of n-TiO<sub>2</sub> and n-TiO<sub>2</sub>:Ag samples under different annealing conditions was studied by X-ray photoelectron spectroscopy. The XPS spectra of the Ti2p- and Ag3d-levels were decomposed by the Gauss-Newton method into interconnected components 2p<sub>3/2</sub>/2p<sub>1/2</sub> and 3d<sub>5/2</sub>/3d<sub>3/2</sub> with parameters  $\Delta E = 5.76$  eV;  $I_1/I_2 = 0.5$  and  $\Delta E = 6.0$  eV;  $I_1/I_2 = 0.66$  to take into account the spin-orbit splitting of the pair respectively. The paper presents histograms of the contributions of the components to the Ti2p- and Ag3d-spectra, which vary depending on the degree of doping and annealing conditions for 4 series of samples. According to XPS data, on the surface of EEW nanopowders TiO<sub>2</sub> and TiO<sub>2</sub>:Ag titanium is represented by Ti<sup>3+</sup>- and Ti<sup>4+</sup>- states, silver by Ag<sup>0</sup>-, Ag<sup>1+</sup>- and Ag<sup>2+</sup>- states. In all series of samples, the contribution of the Ti<sup>3+</sup>- state simultaneously increases with an increase in the absolute Ag content, which is a consequence of the lattice distortion through the formation of a surface phase with Ti–O–Ag bonds. Annealing at 300 °C in air leads to an increase in the contribution to the spectra of Ti<sup>4+</sup>- states of  $E_b$ Ti2p<sub>3/2</sub> = 458.3 eV and Ag<sup>1+</sup>- states. Pretreatment of the samples with hydrogen peroxide before annealing leads to an increase in the contribution of oxide-hydroxide phases of titanium and Ag<sup>0</sup>- states. Annealing of the samples at 300 °C in argon with pretreatment with hydrogen peroxide leads to an increase in the contribution to the spectra of Ti<sup>4+</sup>- states with  $E_b$ Ti2p<sub>3/2</sub> = 458.8 eV, oxide-hydroxide phases of titanium and Ag<sup>0</sup>. It has been found that the direction of redox processes on the surface of n-TiO<sub>2</sub> after the action of H<sub>2</sub>O<sub>2</sub> and subsequent annealing in air depends on the state of hydration of the original nanopowders.*

**Keywords:** n-TiO<sub>2</sub>, n-TiO<sub>2</sub>:Ag, X-ray photoelectron spectroscopy, electric explosion of wires

### INTRODUCTION

Electric explosion of wires (EEW) is a promising technology for the synthesis of TiO<sub>2</sub> nanopowders for photocatalysis. Due to the nonequilibrium state of the EEW process, TiO<sub>2</sub> nanopowders have significant photocatalytic activity, which is associated with a high density of catalytically active centers [1]. In this work, for the first time by the EEW method, TiO<sub>2</sub> was doped with silver during the explosion. Doping with silver makes it possible to optimize the photo- and electrocatalytic characteristics of n-TiO<sub>2</sub> nanopowders [2–8]. Important for the practical applications of electro-explosive n-TiO<sub>2</sub> nanopowders is the study of the effect electronic structure of hydrogen peroxide, which is used as a surface modifier on the surface.

### EXPERIMENT AND DISCUSSION OF THE RESULTS

Powders n-TiO<sub>2</sub>, n-TiO<sub>2</sub>:3 %Ag and n-TiO<sub>2</sub>:5 wt. %Ag were synthesized by the EEW method in a dry air atmosphere by a Ti/Ag<sub>2</sub>O explosion. The explosion energy was equal to  $E = 3.1 \cdot E_s$ , where  $E_s$  is the sublimation energy Ti. The aim of the study is to find by the XPS method the values of the Ti<sup>3+</sup>/Ti<sup>4+</sup>, Ag<sup>0</sup>/Ag<sup>1+</sup>/Ag<sup>2+</sup>, and Ag/Ti ratios depending on the annealing conditions and methods for modifying the sample surface using hydrogen peroxide. The charge states of metals and the relative content of the doping element are the main characteristics of the surface of sensors, photo- and electrocatalysts. Obtaining this information makes it possible to optimize the stages of catalysts synthesis and makes it

possible to carry out controlled synthesis of  $n\text{-TiO}_2$ . The formation of mesoporous nanofilms based on  $n\text{-TiO}_2$  and  $n\text{-TiO}_2\text{/Ag}$  was an intermediate stage in the development of an active element for a gas sensor. The films were 10×10 mm in size and were homogeneous in the nano and macro ranges. An important parameter of films is their nanodispersed structure. The resulting films can be used in photo- and electrocatalysis.

The electronic structure of the  $n\text{-TiO}_2$  and  $n\text{-TiO}_2\text{:Ag}$  was studied by X-ray photoelectron spectroscopy (XPS) using a spectrometer with an energy analyzer PHOIBOS-100\_SPECS ( $E\text{ MgK} = 1253.6\text{ eV}$ ,  $P = 300\text{ W}$ ) [9]. The accuracy of determining the maximum of  $\text{Ti}2p_{3/2}$ -line was  $\pm 0.05\text{ eV}$ , the working vacuum in the chamber was  $1\cdot10^{-10}\text{ Pa}$ , the samples were applied to aluminum substrates measuring 10×10 mm. The samples  $n\text{-TiO}_2\text{:Ag}$  were

annealed at  $300\text{ }^\circ\text{C}$  in air or argon. The annealing temperature was limited in order to inhibit the desorption of silver. Some samples before annealing were in contact with hydrogen peroxide (10 min;  $T = 90\text{ }^\circ\text{C}$ ). Sample 21 series 7 was hydrated for 3 h in humid air at room temperature (Table 1).

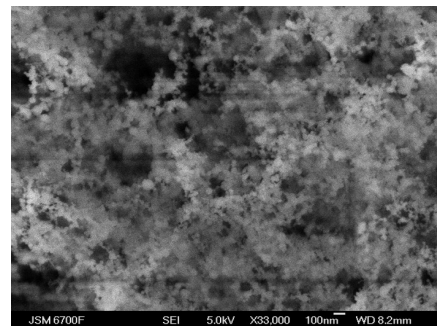


**Fig. 1.** Electron microscopic image of the film of electroexplosive  $\text{TiO}_2$

**Table 1.** List of samples and annealing conditions

Series of samples/ annealing conditions	Number/sample
Series 1 Initial nanopowders	1. $\text{TiO}_2$ 2. $\text{TiO}_2\text{:Ag3 \%}$ 3. $\text{TiO}_2\text{:Ag5 \%}$
Series 2 Annealing in air at $300\text{ }^\circ\text{C}$ for 45 min	4. $\text{TiO}_2$ 5. $\text{TiO}_2\text{:Ag3 \%}$ 6. $\text{TiO}_2\text{:Ag5 \%}$
Series 3 $\text{H}_2\text{O}_2$ treatment followed by annealing in air at $300\text{ }^\circ\text{C}$ for 45 min	7. $\text{TiO}_2$ 8. $\text{TiO}_2\text{:Ag3 \%}$ 9. $\text{TiO}_2\text{:Ag5 \%}$
Series 4 Treatment with $\text{H}_2\text{O}_2$ followed by annealing in Ar at $300\text{ }^\circ\text{C}$ for 45 min	10. $\text{TiO}_2$ 11. $\text{TiO}_2\text{:Ag3 \%}$ 12. $\text{TiO}_2\text{:Ag5 \%}$
Series 5 Annealing in air at $450\text{ }^\circ\text{C}$ for 45 min	13. $\text{TiO}_2$ 14. $\text{TiO}_2\text{:Ag3 \%}$ 15. $\text{TiO}_2\text{:Ag5 \%}$
Series 6 Annealing in Ar at $450\text{ }^\circ\text{C}$ for 45 min	16. $\text{TiO}_2$ 17. $\text{TiO}_2\text{:Ag3 \%}$ 18. $\text{TiO}_2\text{:Ag5 \%}$

The effect of annealing at  $300\text{ }^\circ\text{C}$  in air and argon with preliminary contact with hydrogen peroxide of a part of the samples on the phase composition of their surface was studied. In Fig. 1 the SEM image of a mesoporous film from electroexplosive  $\text{TiO}_2$  is presented.

The spectra of  $\text{Ti}2p$ - and  $\text{Ag}3d$ - levels were decomposed into interconnected components  $2p_{3/2}/2p_{1/2}$  and  $3d_{5/2}/3d_{3/2}$  with the parameters

$\Delta E = 5.76\text{ eV}$ ;  $I_1/I_2 = 0.5$  and  $\Delta E = 6.0\text{ eV}$ ;  $I_1/I_2 = 0.66$  to take into account the spin-orbit splitting of the pair respectively. The decomposition was carried out by the Gauss-Newton method in the mode of bound parameters. The intensity of the components and their binding energy varied. The width of the components and the ratio of the contributions of the Gauss-Lorentz distributions during the

decomposition of the spectra were fixed. The area of the components was determined after subtracting the background by the Shirley method [10–12]. The integral intensities of the components thus obtained are proportional to the content in the samples of non-equivalent titanium and silver ions.

In Figs. 2–3 the  $Ti2p$ - and  $Ag3d$ - spectra of the series 1 initial nanopowders decomposed into components are presented.

In Figs. 4–5 histograms of relative contributions of components of  $Ti2p$ - and  $Ag3d$ -spectra, respectively, for all series of samples of  $TiO_2$ ,  $TiO_2$ :3%Ag,  $TiO_2$ :5 %Ag are presented.

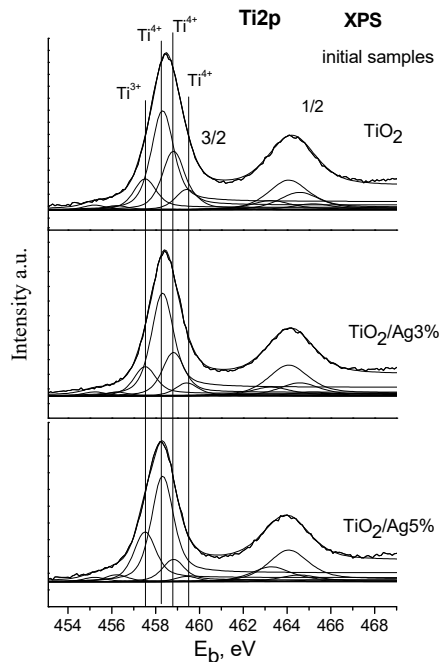


**Fig. 2.** Decomposed into components  $Ti2p$ - spectra of  $TiO_2$ ,  $TiO_2$ :3%Ag,  $TiO_2$ :5%Ag (samples 1-3 series 1)

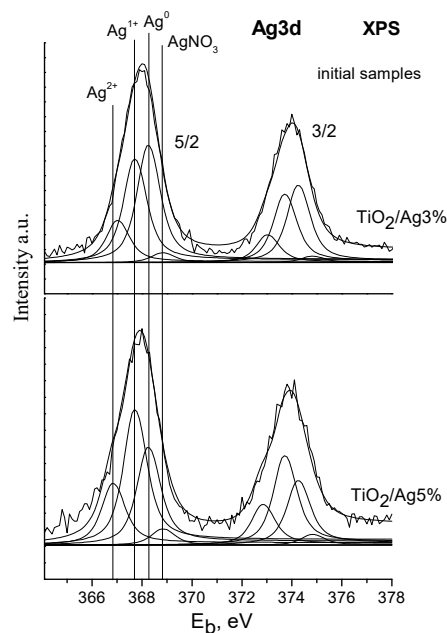


**Fig. 3.** Decomposed into components  $Ag3d$  spectra of  $TiO_2$ :3%Ag,  $TiO_2$ :5%Ag (samples 2-3 series 1)

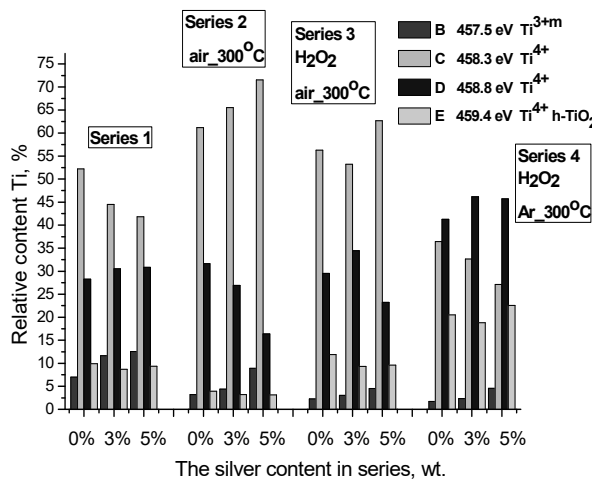


**Fig. 4.** Rrelative integral intensities of the components of the  $\text{Ti}2p$ - line of the samples  $\text{TiO}_2$ ,  $\text{TiO}_2:3\%$ Ag,  $\text{TiO}_2:5\%$ Ag series 1–4

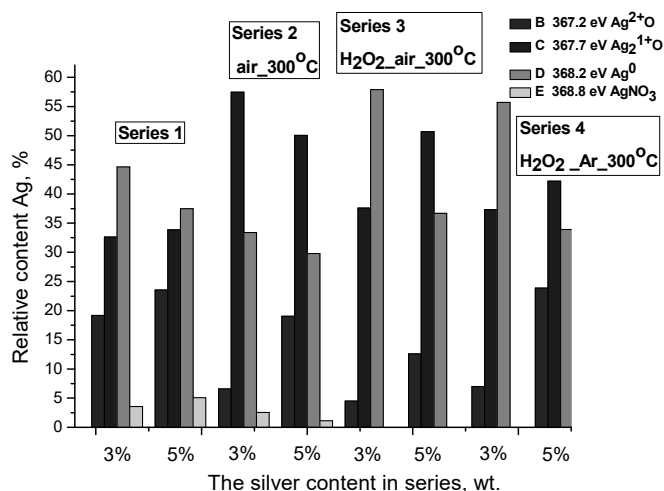


**Fig. 5.** Relative integral intensities of the components of the  $\text{Ag}3d$ - line of samples  $\text{TiO}_2:3\%$ Ag,  $\text{TiO}_2:5\%$ Ag series 1–4

Analysis of the phase composition of the surface of electroexplosive nanopowders  $\text{TiO}_2:\text{Ag}$  depending on the degree of their doping and annealing conditions was carried out on a series of samples:

**Series 1.** The main feature of the initial nanopowders of series 1 (Fig. 4) is a significant content of  $\text{Ti}^{3+}$ - states with  $E_b\text{Ti}2p_{3/2} = 457.5$  eV [13], which indicates both a high degree of surface defects and the formation of  $\text{Ti}-\text{O}-\text{Ag}$  bond [6]. The contribution from  $E_b\text{Ti}2p_{3/2} = 458.3$  eV and from  $E_b\text{Ti}2p_{3/2} = 458.8$  eV, according to [14], are related to  $\text{Ti}^{4+}$ - states of oxide phases. The signal in the  $E_b\text{Ti}2p_{3/2} = 459.4$  eV region corresponds to the  $\text{Ti}^{4+}$  states of the oxide-hydroxide phases of titanium. From Fig. 4. it is seen that when doped

in the samples of series 1, the relative contents of  $\text{Ti}^{3+}$ - states increase, mainly due to  $\text{Ti}^{4+}$ - states with  $E_b\text{Ti}2p_{3/2} = 458.3$  eV.

The components on the spectra of the  $\text{Ag}3d$ -line (Fig. 5) with  $E_b\text{Ag}3d_{5/2} = 367.2$ , 367.7 and 368.2 eV are associated with  $\text{Ag}^{2+}$ -,  $\text{Ag}^{1+}$ - and  $\text{Ag}^0$ -silver states, respectively [12, 15–16].

As the content of the doping element increases, the  $\text{Ti}^{3+}$ - states increase (Fig. 4), which indicates the insertion of silver into the  $\text{TiO}_2$  lattice and the formation of  $\text{Ti}-\text{O}-\text{Ag}$  bonds. Substitution of  $\text{Ti}^{4+}$ - ions by  $\text{Ag}^{n+}$ - ions, taking into account the difference of their ionic radii ( $R_{\text{Ti}^{4+}} = 0.75\text{\AA}$ ;  $R_{\text{Ag}^{2+}} = 1.08\text{\AA}$ ;  $R_{\text{Ag}^{1+}} = 1.29\text{\AA}$ ), is possible only on the surface of nanoparticles due to structural relaxation, for example, the appearance of  $\text{Ti}^{3+}$ - states.

In the  $E_b Ag3d_{5/2} = 368.8$  eV region, there is a small contribution that can be related to the synthesis explosion of the  $AgNO_3$  phase in an air [16–17].

In general, for electroexplosive nanopowders of series 1, the dominant in the phase distribution of the parent metal is the content of  $Ti^{4+}$ - states with  $E_b Ti2p_{3/2} = 458.3$  eV, which may be associated with the anatase phase [13–15, 18–20]. In the sample with 5%Ag (Fig. 4) the relative content of  $Ti^{3+}$ - states is maximum. The content of metallic silver is dominant in the phase distribution of the doping metal, and the relative content of  $Ag^0$  is maximum in samples with 3%Ag (Fig. 5).

**Series 2.** Annealing in air leads to a linear increase on the surface of samples of relative content of  $Ti^{4+}$ - states with  $E_b = 458.3$  eV, which is associated with the anatase phase. Also during doping with increasing silver content, the content of  $Ti^{3+}$ - states increases (Fig. 4). According to the results of the decomposition of  $Ag3d$ -spectra, a relative decrease in the content of metallic silver in this series of samples is observed due to its oxidation to  $Ag_2O$  (Fig. 5).

**Series 3.** Treatment with hydrogen peroxide of samples before their annealing in air leads to an increase for all samples of the contribution of oxide-hydroxide phases with  $E_b = 459.4$  eV ( $Ti^{4+}$ ). The relative content of  $Ti^{4+}$ - states of the oxide phase with  $E_b Ti2p_{3/2} = 458.8$  eV, which can be associated with rutile [13]. However, the signal in the region  $Ti2p_{3/2} = 458.8$  eV can also belong to the hydrated oxide phase  $TiO_2-OH$ . The relative content of  $Ti^{4+}$ - states with  $E_b = 458.3$  eV decreases in comparison with series 2, but remains dominant. The content of  $Ti^{3+}$ - states also decreases.

According to  $Ag3d$  spectra, after annealing there is a reduction of part of the oxide phases of silver to metal. In the sample  $TiO_2:3\%$ Ag, the relative content of metallic silver in comparison with the oxide phases becomes dominant and the largest among all series (Fig. 5).

**Series 4.** Hydrogen peroxide treatment of samples of  $TiO_2$  and  $TiO_2:Ag$  before annealing and change of air environment during annealing to argon leads to the dominance of the phase with  $E_b = 458.8$  eV ( $Ti^{4+}$ , rutile) and increase the contribution of oxide-hydroxide phases of titanium ( $Ti^{4+}$ ,  $E_b = 459.4$  eV) for all samples of the series (Fig. 4). In the sample  $TiO_2:3\%$ Ag, the relative content of metallic silver is

dominant. As in the previous case, this is a consequence of the reduction of the surface oxide phase of  $Ag_2O$  under the action of  $H_2O_2$  before annealing.

In general, the relative contents of  $Ti^{3+}$ -states in  $TiO_2:Ag$  increase during doping. Annealing in air and argon of nanopowders in contact with hydrogen peroxide leads to an increase in the oxide-hydroxide phases of titanium with the simultaneous reduction of some oxides of silver to metal.

In each series of samples, as the silver content increases during doping, the content of  $Ti^{3+}$ - states simultaneously increases, which may indicate the formation of a surface phase with  $Ti-O-Ag$  bonds.

For all series of samples, the maximum content in samples with 5%Ag is the content of  $Ti^{3+}$ - states, and in samples with 3%Ag - the relative content of  $Ag^0$  (Figs. 4–5).

Fig. 6 shows the total silver content ( $Ag/Ti$ , wt.) on the surface of  $TiO_2:Ag$  nanopowders for various series.

**Series 1.** In electroexplosive nanopowders, the total silver content on the surface always exceeds the mass values specified in the synthesis. This can be explained by the fact that silver can form metallic and oxide phases only on the surface of already formed  $TiO_2$  nanoparticles and at the interfaces of agglomerates due to a significant difference in ionic radii and lower melting point values.

**Series 2.** Upon annealing at 300 °C in air, the  $Ag/Ti$  value for the samples  $TiO_2:3\%$ Ag and  $TiO_2:5\%$ Ag (series 2, Fig. 6) increases, respectively, to 5–7%, which is the result of the action of the processes of silver segregation onto the surface of the agglomerates. According to the XPS data, after annealing at 300 °C in air, the main phases on the surface of the nanopowder are silver oxides.

**Series 3.** After the action of  $H_2O_2$  and further annealing in the samples of series 3 (as compared with samples of series 2), the total silver content  $Ag/Ti$  and, (Fig. 6) decreases to 3–5% (with a simultaneous increase (Fig. 5) of the relative content of metallic silver).

That is, a decrease in the value of  $Ag/Ti$  was recorded and, although the reducing effect of  $H_2O_2$  on  $Ag_2O$  and  $AgO$  should lead to an increase in  $Ag/Ti$  and due to a decrease in the content of silver oxides with a low desorption temperature. This can be caused by the

destruction under the action of  $H_2O_2$  of the interface in the agglomerates of silver oxides, a decrease in their size and growth of the specific surface, and as a consequence, the activation of oxidation and desorption processes.

**Series 4.** The largest accumulation of silver (up to 9–12 %) on the surface of  $TiO_2:Ag$

nanopowders occurs during their contact with  $H_2O_2$  and annealing in argon (series 4), which is associated with inhibition of oxidation processes and, accordingly, desorption. According to the XPS data, after annealing, in the samples of series 4, the content of metallic silver in relation to the oxide phases is maximum (Fig. 5).

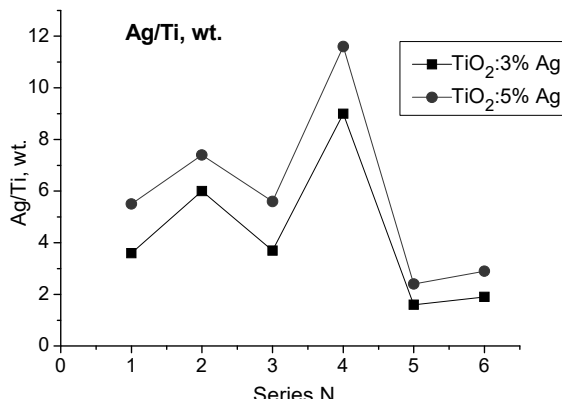


**Fig. 6.** The total content of silver  $Ag/Ti$ , wt. on the surface of  $TiO_2:3\%Ag$  and  $TiO_2:5\%Ag$  nanopowders, depending on the annealing conditions

With an increase in the annealing temperature to 450 °C (series 5–6), which is higher than the desorption temperature of the  $Ag_2O$  and  $AgO$  oxides ( $T_{desorp} \sim 250$ –350 °C), regardless of the gas medium, the total silver content on the surface within a short time sharply decreases to 2–3 % ( $Ag/Ti$ , Fig. 6).

Thus, in the range of annealing of 300–350 °C, should be expected enrichment of the surface with silver as a result of segregation processes. With an increase in the  $TiO_2:Ag$  annealing temperature (for example, up to 400–450 °C in order to form the anatase phase), the processes of desorption of silver oxides should be taken into account.

In the process of studying the effect of hydrogen peroxide on electroexplosive  $TiO_2$  nanopowders, a change in the direction of redox processes on their surface was established. Fig. 7 shows the dependence of the phase composition of the surface of series 7 (Table 2) annealed  $TiO_2$  nanopowders on their preliminary treatment with hydrogen peroxide and the state of the surface.

Fig. 7 shows that the state of the surface of the samples before their contact with hydrogen peroxide and subsequent annealing in air affects the ratio of nonequivalent states of titanium.

In the sample  $TiO_2$  (20), dried and modified with hydrogen peroxide before annealing, compared with the initial sample  $TiO_2$  (19) increases the content of  $Ti^{3+}$ -states and  $Ti^{4+}$ -states with  $E_b = 458.3$  eV, which bind to the anatase phase and decreases the content of  $Ti^{4+}$ -states that bind to the rutile phase and oxide-hydroxide phases.

In the sample  $TiO_2$  (21), the surface of which before contact with  $H_2O_2$  was hydrated, the content of  $Ti^{3+}$ -states decreases, the content of  $Ti^{4+}$ -states that bind to the rutile phase becomes dominant and the content of titanium oxide-hydroxide phases increases.

Thus, the hydration degree of  $TiO_2$  nanopowders treated with hydrogen peroxide before annealing in air determines the direction of redox processes on their surface.

**Table 2.** List of samples and annealing conditions

Series of samples/ annealing conditions	Number/sample
Series 7	19. $TiO_2$ dried sample
Annealing in air at 450 °C for 45 min	20. $TiO_2$ , dried sample, $H_2O_2$ treatment 21. $TiO_2$ , hydrated sample, $H_2O_2$ treatment

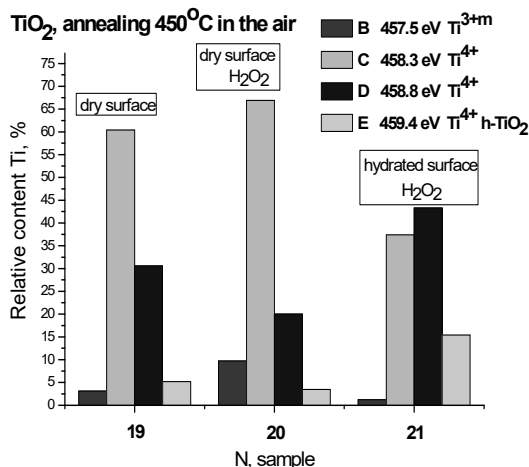


**Fig. 7.** Relative integral intensities of  $Ti2p$ -line components for  $TiO_2$  nanopowders of series 7 annealed at 450 °C in air: sample 19 - dry surface, no treatment before annealing; sample 20 - treatment with hydrogen peroxide dry surface before annealing; sample 21 - treatment with hydrogen peroxide hydrated surface before annealing

## CONCLUSIONS

According to the XPS data, on the surface of electroexplosive nanopowders  $TiO_2$ ,  $TiO_2:Ag$  titanium is presented by  $Ti^{3+}$ - and  $Ti^{4+}$ - states, silver by  $Ag^0$ -,  $Ag^{1+}$ - and  $Ag^{2+}$ - states.

In all the series of samples with increasing absolute content of Ag simultaneously increases the contribution of  $Ti^{3+}$ - states, which is a consequence of the lattice distortion due to the formation of the surface phase with the  $Ti-O-Ag$  bonds.

Annealing at 300 °C in air increases the contribution to the spectra of  $Ti^{4+}$ - states, which are associated with the anatase phase and the

contribution of  $Ag^{1+}$ - states. Pretreatment of samples with hydrogen peroxide before annealing leads to an increase in the contribution of oxide-hydroxide phases of titanium and  $Ag^0$ -states.

Annealing of the samples at 300 °C in argon with pretreatment with hydrogen peroxide leads to an increase in the contribution of the rutile phase, oxide-hydroxide phases of titanium and  $Ag^0$ -states.

The direction of redox processes on the surface of  $n-TiO_2$  after the action of  $H_2O_2$  and subsequent annealing in air depends on the state of hydration of the initial nanopowders.

## Дослідження методом РФС поверхні нанопорошків $TiO_2:Ag$

**О.М. Кордубан, Т.В. Крищук, В.О. Кандиба, В.В. Трачевський**

Інститут загальної та неорганічної хімії ім. В.І. Вернадського Національної академії наук України  
просп. Академіка Палладіна, 32/34, Київ, 03680, Україна, tarkry@ukr.net

*Elettra – Sincrotrone Trieste SCoP  
SS14-km 163.5 in Area Science Park, Basovizza, 34012, Trieste, Italy*

*Технічний центр Національної академії наук України  
бул. Покровська, 13, Київ, 04070, Україна*

*Методом електричного вибуху провідників (ЕВП) синтезовано нанопорошки  $n-TiO_2$  та  $n-TiO_2:Ag$ . Легування нанопорошків відбувалось під час вибуху титанового дроту, на поверхню якого було нанесено шар  $Ag_2O$  відповідної маси. Енергія вибуху дорівнювала  $E = 3.1 \cdot E_c$ , де  $E_c$  – енергія сублімації металу. На основі синтезованих нанопорошків сформовано мезопорувати  $n-TiO_2$  та  $n-TiO_2:Ag$  плівки. Методом рентгенівської*

фотоелектронної спектроскопії досліджено фазовий склад поверхні кількох серій  $n\text{-TiO}_2$  та  $n\text{-TiO}_2\text{:Ag}$  зразків при різних умовах відпалу. РФС-спектри  $Ti2p$ - і  $Ag3d$ -рівнів були розкладені методом Гаусса-Ньютона на зв'язані між собою для врахування спін-орбітального розщеплення пари компонент  $2p_{3/2}/2p_{1/2}$  і  $3d_{5/2}/3d_{3/2}$  з параметрами  $\Delta E = 5.76$  eВ;  $I_1/I_2 = 0.5$  та  $\Delta E = 6.0$  eВ;  $I_1/I_2 = 0.66$  відповідно. В роботі приведені гістограми вкладів компонент у  $Ti2p$ - та  $Ag3d$ -спектри, які змінюються в залежності від ступеня легування та умов відпалу для 4 серій зразків. За даними РФС на поверхні ЕВП - нанопорошків  $n\text{-TiO}_2$  та  $n\text{-TiO}_2\text{:Ag}$  титан представлений  $Ti^{3+}$ - та  $Ti^{4+}$ - станами, срібло -  $Ag^0$ ,  $Ag^{1+}$ - та  $Ag^{2+}$ - станами. В усіх серіях зразків зі збільшенням абсолютноого вмісту Ag одночасно зростає вклад  $Ti^{3+}$ - станів, що є наслідком викривлення гратки через формування поверхневої фази зі зв'язком  $Ti-O-Ag$ . Відпал при 300 °C в повітрі призводить до зростання вкладу в спектри  $Ti^{4+}$ - станів  $E_{ce}Ti2p_{3/2} = 458.3$  eВ та  $Ag^{1+}$ - станів. Попередня обробка зразків перекисом водню перед їх відпалом призводить до збільшення вкладу оксидно-гідроксидних фаз титану та  $Ag^0$ - станів. Відпал зразків при 300 °C в аргоні з попередньою обробкою перекисом водню призводить до збільшення вкладу в спектри  $Ti^{4+}$ - станів з  $E_{ce}Ti2p_{3/2} = 458.8$  eВ, оксидно-гідроксидних фаз титану та  $Ag^0$ . Установлено, що напрямок окиснювано-відновлювальних процесів на поверхні  $n\text{-TiO}_2$  після дії  $H_2O_2$  та подальшого відпалу в повітрі залежить від стану гідратованості вихідних нанопорошків.

**Ключові слова:**  $n\text{-TiO}_2$ ,  $n\text{-TiO}_2\text{:Ag}$ , рентгенівська фотоелектронна спектроскопія, електричний вибух провідників

## Исследование методом РФС поверхности нанопорошков $\text{TiO}_2\text{:Ag}$

А.М. Кордубан, Т.В. Крищук, В.А. Кандыба, В.В. Трачевский

Институт общей и неорганической химии им. В.И. Вернадского Национальной академии наук Украины  
просп. Академика Палладина, 32/34, Киев, 03680, Украина, tarkry@ukr.net

Elettra – Sincrotrone Trieste SCpA  
SS14-km 163.5 in Area Science Park, Basovizza, 34012, Trieste, Italy  
Технический центр Национальной академии наук Украины  
ул. Покровская, 13, Киев, 04070, Украина

Методом электрического взрыва проводников (ЭВП) синтезированы нанопорошки  $n\text{-TiO}_2$  и  $n\text{-TiO}_2\text{:Ag}$ . Легирование нанопорошков происходило при взрыве титановой проволоки, на поверхность которой был нанесен слой  $Ag_2O$  соответствующей массы. Энергия взрыва была равна  $E = 3.1E_c$ , где  $E_c$  – энергия сублимации металла. На основе синтезированных нанопорошков сформированы мезопористые  $n\text{-TiO}_2$  и  $n\text{-TiO}_2\text{:Ag}$  пленки. Методом рентгеновской фотоэлектронной спектроскопии исследован фазовый состав поверхности нескольких серий  $n\text{-TiO}_2$  и  $n\text{-TiO}_2\text{:Ag}$  образцов при различных условиях отжига. РФС-спектры  $Ti2p$ - и  $Ag3d$ - уровней были разложены методом Гаусса-Ньютона на связанные между собой для учета спин-орбитального расщепления пары компонент  $2p_{3/2}/2p_{1/2}$  и  $3d_{5/2}/3d_{3/2}$  с параметрами  $\Delta E = 5.76$  эВ;  $I_1/I_2 = 0.5$  и  $\Delta E = 6.0$  эВ;  $I_1/I_2 = 0.66$  соответственно. В работе приведены гистограммы вкладов компонент в  $Ti2p$ - и  $Ag3d$ -спектры, которые меняются в зависимости от степени легирования и условий отжига для 4 серий образцов. По данным РФС на поверхности ЭВП - нанопорошков  $TiO_2$  и  $TiO_2\text{:Ag}$  титан представлен  $Ti^{3+}$ - и  $Ti^{4+}$ - состояниями, серебро  $Ag^0$ ,  $Ag^{1+}$ - и  $Ag^{2+}$ - состояниями. Во всех сериях образцов с увеличением абсолютноного содержания Ag одновременно возрастает вклад  $Ti^{3+}$ - состояний, что является следствием искажения решетки через формирование поверхностной фазы со связью  $Ti-O-Ag$ . Отжиг при 300 °C в воздухе приводит к росту вклада в спектры  $Ti^{4+}$ - состояний  $E_{ce}Ti2p_{3/2} = 458.3$  эВ и  $Ag^{1+}$ - состояний. Предварительная обработка образцов перекисью водорода перед их отжигом приводит к увеличению вклада оксидно-гидроксидных фаз титана и  $Ag^0$ - состояний. Отжиг образцов при 300 °C в аргоне с предварительной обработкой перекисью водорода приводит к увеличению вклада в спектры  $Ti^{4+}$ - состояний с  $E_{ce}Ti2p_{3/2} = 458.8$  эВ, оксидно-гидроксидных фаз титана и  $Ag^0$ . Установлено, что направление окислительно-восстановительных процессов на поверхности  $n\text{-TiO}_2$  после действия  $H_2O_2$  и дальнейшего отжига в воздухе зависит от состояния гидратированности выходных нанопорошков.

**Ключевые слова:**  $n\text{-TiO}_2$ ,  $n\text{-TiO}_2\text{:Ag}$ , рентгеновская фотозелектронная спектроскопия, электрический взрыв проводников

## REFERENCES

1. Ranjan P., Nakagawa S., Suematsu H., Sarathi R. Synthesis and photocatalytic activity of anatase/rutile  $TiO_2$  nanoparticles by wire explosion process. *INAE Lett.* 2018. **3**(4): 189.
2. Zhao Z., Hwang S.H., Jeon S., Hwang B., Jung J.-Yu., Lee J., Park S.-Hu Three-dimensional plasmonic  $Ag/TiO_2$  nanocomposite architectures on flexible substrates for visible-light photocatalytic activity. *Sci. Rep.* 2017. **7**: 8915.
3. Diesen V., Jonsson M. Formation of  $H_2O_2$  in  $TiO_2$  photocatalysis of oxygenated and deoxygenated aqueous systems: a probe for photocatalytically produced hydroxyl radicals. *J. Phys. Chem. C.* 2014. **118**(19): 10083.
4. Wu Z., Guo K., Cao S., Yao W., Piao L. Synergetic catalysis enhancement between  $H_2O_2$  and  $TiO_2$  with single-electron-trapped oxygen vacancy. *Nano Res.* 2020. **13**: 551.
5. Benkoula S., Sublemonier O., Patanen M., Nicolas C., Sirotti F., Naitabdi A., Gaie-Levrel F., Antonsson E., Aureau D., Ouf F.-X., Wada Sh.-I., Etcheberry A., Ueda K., Miron C. Water adsorption on  $TiO_2$  surfaces probed by soft X-ray spectroscopies: bulk materials vs. isolated nanoparticles. *Sci. Rep.* 2015. **5**: 15088.
6. Gogoi D., Namdeo A., Golder A.K., Peela N.R. Ag-doped  $TiO_2$  photocatalysts with effective charge transfer for highly efficient hydrogen production through water splitting. *Int. J. Hydrogen Energy.* 2020. **45**(4): 2729.
7. Shwetharani R., Sakar M., Fernando C.A.N., Binas V., GeethaBalakrishna R. Recent advances and strategies applied to tailor energy levels, active sites and electron mobility in titania and its doped/composite analogues for hydrogen evolution in sunlight. *Catal. Sci. Technol.* 2019. **9**(1): 12.
8. Cao Y., Tan H., Shi T., Tang T., Li J. Preparation of Ag-doped  $TiO_2$  nanoparticles for photocatalytic degradation of acetamiprid in water. *J. Chem. Technol. Biotechnol.* 2008. **83**(4): 546.
9. Shpak A.P., Korduban A.M., Medvedskij M.M., Kandyba V.O. XPS studies of active elements surface of gas sensors based on  $WO_{3-x}$  nanoparticles. *J. Electron Spectrosc. Relat. Phenom.* 2007. **156–158**: 172.
10. Briggs D., Seach M.P. *Practical Surface Analysis by Auger and X-ray Photoelectron Spectroscopy*. (Chichester – New York: John Wiley & Sons Ltd., 1983).
11. Wagner C.D., Moulder J.F., Davis L.E., Riggs W.M. *Handbook of X-ray Photoelectron Spectroscopy*. (New York: Perkin-Elmer Corporation, 1979).
12. Nefedov V.I. *Roentgenoelectronic Spectroscopy of Chemical Compounds*. (Moscow: Khimiya, 1984). [in Russian].
13. Satoh N., Nakashima T., Kamikura K., Yamamoto K. Quantum size effect in  $TiO_2$  nanoparticles prepared by finely controlled metal assembly on dendrimer templates. *Nat. Nanotechnol.* 2008. **3**: 106.
14. Sikdar S., Pathak S., Ghorai T.K. Aqueous phase photodegradation of rhodamine B and p-nitrophenol destruction using titania based nanocomposites. *Adv. Mater. Lett.* 2015. **6**(10): 867.
15. Wint T.H.M., Smith M.F., Chanlek N., Chen F., Oo T.Z., Songsiririthigul P. Physical origin of diminishing photocatalytic efficiency for recycled  $TiO_2$  nanotubes and Ag-loaded  $TiO_2$  nanotubes in organic aqueous solution. *Catalysts.* 2020. **10**(7): 737.
16. Ferraria A.M., Carapeto A.P., Botelho do Rego A.M. X-ray photoelectron spectroscopy: silver salts revisited. *Vacuum.* 2012. **86**(12): 1988.
17. Thomas S., Durand D., Chassenieux C., Jyotishkumar P. *Handbook of Biopolymer-Based Materials: From Blends and Composites to Gels and Complex Networks*. (John Wiley & Sons, 2013). P. 61.
18. Agirseven O., Rivella D.T.Jr., Haggerty J.E.S., Berry P.O., Diffendaffer K., Patterson A., Kreb J., Mangum J.S., Gorman B.P., Perkins J.D., Chen B.R., Schelhas L.T., Tate J. Crystallization of  $TiO_2$  polymorphs from RF-sputtered, amorphous thin-film precursors. *AIP Adv.* 2020. **10**(2): 025109.
19. Eremenko A., Smirnova N., Gnatiuk I., Linnik O., Vityuk N., Mukha Y., Korduban A. Silver and Gold Nanoparticles on Sol-Gel  $TiO_2$ ,  $ZrO_2$ ,  $SiO_2$  Surfaces: Optical Spectra, Photocatalytic Activity, Bactericide Properties. In: *Nanocomposites and Polymers with Analytical Methods*. Chapter 3: Composite Materials. 2011. P. 51.
20. Linnik O., Petrik I., Smirnova N., Kandyba V., Korduban A.M., Eremenko A., Socol G., Stefan N., Ristoscu C., Mihailescu I.N., Sutan C., Viorel M., Djokic V., Janackovic D.  $TiO_2/ZrO_2$  thin films synthesized by PLD in low pressure N-, C- and/or O-containing gases: structural, optical and photocatalytic properties. *Digest Journal of Nanomaterials and Biostructures.* 2012. **7**(3): 1343.

Received 02.11.2020, accepted 25.11.2020